Analysis of the in-plane magnetic anisotropy in amorphous ribbons obtained by torque magnetometry

M. Tejedor, J. A. García, J. Carrizo, L. Elbaile,[a] and J. D. Santos
Departamento de Física, Universidad de Oviedo, Calvo Sotelo S/N, 33007 Oviedo, Spain

J. Mira and J. Rivas
Departamento de Física Aplicada, Universidade de Santiago de Compostela, 15706 Santiago de Compostela, Spain

(Received 8 December 1998; accepted for publication 11 May 1999)

The evolutions of the uniaxial torque and magnetization with the applied magnetic field allow us to discriminate the sources of in-plane magnetic anisotropy in amorphous ribbons. In order to determine the magnetic anisotropy sources, a simple model has been developed for an inhomogeneous material. We apply this model to explain the quite different behavior observed in the evolution of the uniaxial torque amplitude with the applied magnetic field of two commercial Co-based amorphous alloys. © *1999 American Institute of Physics.* [S0021-8979(99)07416-2]

I. INTRODUCTION

Amorphous magnetic ribbons obtained by rapid solidification show in-plane magnetic anisotropy. Since these materials lack of long-range order, the most probable causes of this anisotropy are shape factors or stresses developed around irregularities such as surface roughness, microholes, crystalline precipitates, composition fluctuations, or overstrained zones,[1,2] residual stresses frozen in the material after the solidification process,[3] and directional order originating from the manufacturing process.[4,5] These different sources give rise to anisotropies that affect different regions of the material; residual stresses and directional order would produce magnetic anisotropy influencing the whole material, while the other sources of anisotropy would only affect the small volumes occupied by the irregularities.

Generally, amorphous ribbons are soft magnetic materials and reach saturation magnetization at applied magnetic fields of the order of a few Oersteds. Above these low magnetic fields, the in-plane magnetic anisotropy measured by torque magnetometry should be essentially constant. However, the fact that the measured torques can increase[6] or decrease[7] with the applied magnetic field indicates a lack of magnetic saturation of the entire sample.

Studies of the dependence of the in-plane magnetic anisotropy on the applied field in these materials indicate that the saturation value of this magnitude is reached at hundreds or thousands of Oersteds.[8] This lag between the magnetic field necessary to saturate the magnetization and that needed to saturate the measured in-plane magnetic anisotropy has been interpreted as due to the contribution to the torque of unsaturated imperfections in the sample that occupy a small volume, but produce a high magnetic anisotropy. The magnetization in these zones is only saturated at high applied fields. Nevertheless, due to the small fraction of volume that they occupy, their contribution to the magnetization would be negligible, so the total magnetization saturation is apparently achieved at the low fields mentioned above.

From the dependence of the measured in-plane anisotropy and magnetization on the applied field with different mechanical polishing, electrolytical polishing, and thermal treatments, it is possible clarify the different sources of the in-plane anisotropy and the volumes of the samples affected by them.

In the present article, we study the dependence of the uniaxial torque amplitude T_u on the applied magnetic field H in two different amorphous ribbons. The differences found in the $T_u - H$ curves in both amorphous alloys are explained by means of an approximate model for inhomogeneous samples developed by some of the authors.[8] With this simple model, it is possible to evaluate the anisotropy distribution within the samples. Magnetization curves and torque measurements carried out in the samples after mechanical polishing are also presented in order to corroborate the results.

II. EXPERIMENTAL PROCEDURE

Both of the materials employed in the present article are Co-based magnetic amorphous ribbons with very low magnetostriction in order to avoid the possible stress effects after the mechanical polishing. The first alloy is VITROVAC 6150, which is a trade mark of the German company Vacumschmeltze. It is a 2.5 cm wide and 40 μm thick ribbon, with the following magnetic properties: saturation magnetization $\mu_0 M_s = 1$ T, Curie temperature $T_c = 485\,^{\circ}$C, and saturation magnetostriction $\lambda_s < 2\times10^{-7}$. The second is an amorphous alloy manufactured by the British Goodfellow Corporation of composition $Co_{66}B_{12}Si_{16}Fe_4Mo_2$. It is a 2.0 cm wide and 40 μm thick ribbon, with $\mu_0 M_s = 0.55$ T, $T_c = 250\,^{\circ}$C, and $\lambda_s < 3\times10^{-7}$. The values of the magnetic properties of both samples have been obtained from the catalogues of the firms.

In order to avoid shape effects, nearly perfect circular samples were cut out from the ribbons using a method developed in our laboratory.[9] The diameters of the samples were 10.62 mm for the sample of VITROVAC 6150 and 9.96 mm for $Co_{66}B_{12}Si_{16}Fe_4Mo_2$. Torque measurements

[a]Electronic mail: elbaile@pinon.ccu.uniovi.es

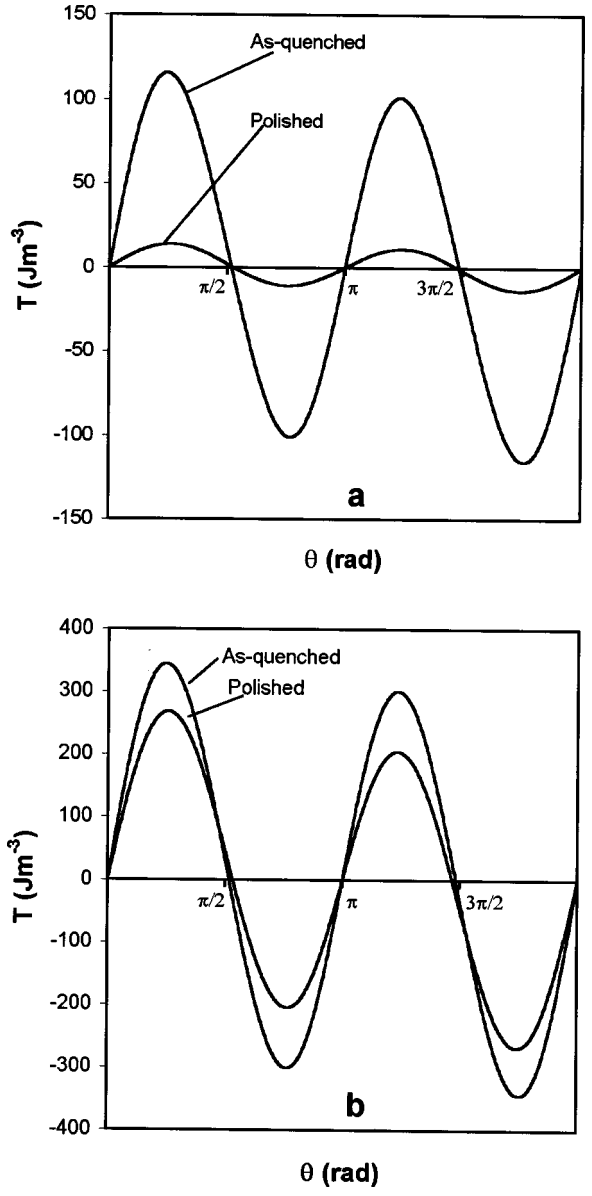

FIG. 1. Torque curves for both the as-quenched and polished states: (a) for $Co_{66}B_{12}Si_{16}Fe_4Mo_2$ and (b) for VITROVAC 6150.

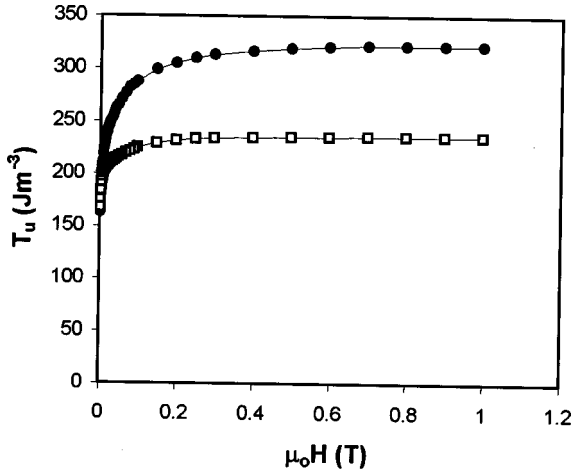

FIG. 2. Evolution of the uniaxial torque amplitude per unit volume T_u with the applied magnetic field for VITROVAC 6150 in the as-quenched state (●) and after the mechanical polishing of its wheel surface (□).

were performed by means of an automatic torque magnetometer ''DMS-1660'' from Digital Measurements Systems and the magnetization curves were measured by the induction method. The mechanical polishing of the samples was carried out with 1 μm grain size allumina. It was performed at random in order to avoid the formation of an oriented roughness that could originate a new magnetic anisotropy in the samples.

III. RESULTS AND DISCUSSION

Figures 1(a) and 1(b) show the typical torque curves obtained for $Co_{66}B_{12}Si_{16}Fe_4Mo_2$ and VITROVAC 6150, respectively, for both as-quenched and polished states.

Figures 2 and 3 show the dependence of the uniaxial torque amplitude per unit volume T_u on the applied magnetic field $\mu_0 H$ for VITROVAC 6150 and $Co_{66}B_{12}Si_{16}Fe_4Mo_2$, respectively. The measurements were carried out in the as-quenched state and then after mechanical polishing of the wheel surface which presents the main contribution to the surface anisotropy. The magnetic anisotropy measured in both samples has the easy axis along the longitudinal direction of the ribbon. The behavior of these curves can be summarized as follows:

(1) For VITROVAC 6150 in the as-quenched state, T_u increases rapidly at low fields. At about 0.1 T, the curve bends forming a knee, then increases slowly and practically saturates at 0.3 T. At this magnetic field, the torque is $T_u = 320\,\mathrm{J\,m^{-3}}$. After mechanical polishing, the curve saturates at about 0.2 T and the maximum value of T_u reached is 236 $\mathrm{J\,m^{-3}}$.

(2) For as-quenched $Co_{66}B_{12}Si_{16}Fe_4Mo_2$, the behavior of T_u is quite different: it increases more slowly and reaches its maximum value of 120 $\mathrm{J\,m^{-3}}$ at 1.0 T. After mechanical polishing, the maximum value is 12.4 $\mathrm{J\,m^{-3}}$ and it is reached at 0.1 T.

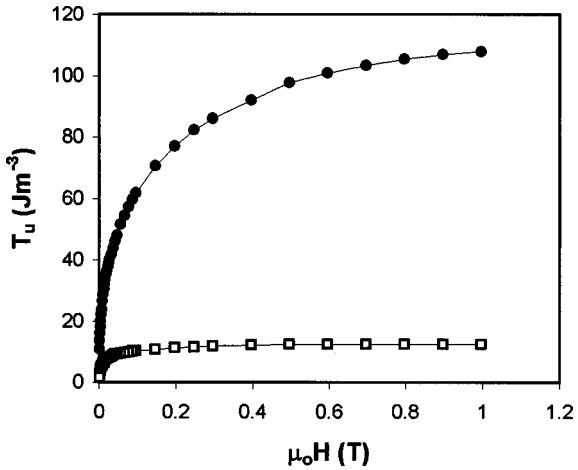

FIG. 3. Evolution of the uniaxial torque amplitude per unit volume T_u with the applied magnetic field for $Co_{66}B_{12}Si_{16}Fe_4Mo_2$ in the as-quenched state (●), and after the mechanical polishing of its wheel surface (□).

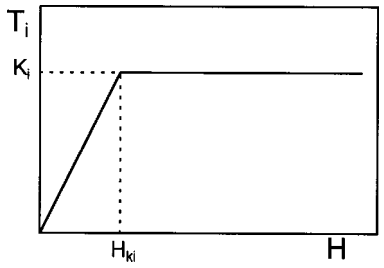

FIG. 4. Linear approximation for the evolution of the uniaxial torque amplitude T_i with the applied magnetic field for one of the regions (ith region) in which the sample is considered to be formed. The maximum torque amplitude K_i is the magnetic anisotropy constant of the region and is reached at the anisotropy field H_{ki}.

Analyzing the behavior of the curves corresponding to the as-quenched state, the sample VITROVAC 6150 shows a greater macroscopic anisotropy than $Co_{66}B_{12}Si_{16}Fe_4Mo_2$ but, nevertheless, its torque amplitude saturates at a very much lower applied magnetic field.

The explanation of this behavior stems from the fact that the macroscopic anisotropy constant is measured as the volume averaged anisotropy energy. It is possible to have a high magnetic anisotropy occupying only a small fraction of the volume of the sample. In this case, the macroscopic anisotropy and the torque measured per unit volume would be small. On the other hand, a low magnetic anisotropy affecting the whole material can produce a greater torque on the sample.

In the same way, if a sample exhibits a low torque amplitude due to the presence of a high magnetic anisotropy in a small fraction of the volume, it is expected that the curve T_u-H saturates only at the high applied magnetic fields at which the strongly anisotropic zones in the material are saturated.

In order to estimate the anisotropy distribution of the two samples and explain the different behavior shown in Figs. 2 and 3 in more detail, we have developed a simple model based on a previous work.[8]

For simplification, we have made the following assumptions:

(1) The sample is formed by an indefinite number of regions that occupy different volume fractions and exhibit different magnetic anisotropies.

(2) In each region, the uniaxial torque amplitude varies linearly with the applied field H, as shown in Fig. 4. The measured anisotropy of the ith region increases linearly until the anisotropy field H_{ki} is reached. Then, the uniaxial torque amplitude T_i reaches the maximum value K_i, which is the magnetic anisotropy constant of the ith region.

Taking Fig. 4 into account, we can obtain the torque amplitude T_i exerted in the ith region as follows:

$$\text{if} \quad H<H_{ki}, \quad \text{then} \quad T_i=\frac{K_i}{H_{ki}}H; \tag{1}$$

$$\text{if} \quad H\geqslant H_{ki}, \quad \text{then} \quad T_i=K_i. \tag{2}$$

Within this linear approximation, T_u-H curves can be considered as formed by a series of linear steps, changing step each time that the saturation of a zone is reached at the field $H=H_{ki}$.

The anisotropy constant of the whole sample K_u can be considered as the volume weighted sum of the contributions of each anisotropy region:

$$K_u=\sum_{i=1}^{n} K_i f_i, \tag{3}$$

where f_i is the volume fraction corresponding to the ith region. The anisotropy constant K_i can be related to the anisotropy field H_{ki} and the saturation magnetization M_s as follows:

$$K_i=\frac{1}{2}\mu_0 M_s H_{ki}. \tag{4}$$

If the sample is still unsaturated at an intermediate field H, it means that the zones with anisotropy field $H_k<H$ are saturated and that there are zones with $H_k>H$ which remain unsaturated.

Similarly, the uniaxial torque amplitude T_u for the whole sample at a field H, with $H_{ki-1}<H<H_{ki}$ can be expressed as

$$T_u=a_i+b_iH=K_1f_1+K_2f_2+\cdots+K_{i-1}f_{i-1}+\left(\frac{K_if_i}{H_{ki}}+\frac{K_{i+1}f_{i+1}}{H_{ki+1}}+\cdots+\frac{K_nf_n}{H_{kn}}\right)H. \tag{5}$$

In this case, the zones $1,2,...,i-1$ are saturated and contribute with constant terms [Eq. (2)] to the total torque amplitude T_u. They constitute the independent term a_i of the straight line. The zones $i,i+1,...,n$ are unsaturated and their contributions [Eq. (1)] are responsible for the slope of the straight line between the fields H_{ki-1} and H_{ki}.

Using the preceding ideas we can evaluate the anisotropy constant and the volume fraction of each anisotropic region. We can consider the applied magnetic field of each measurement as being the anisotropy field of a corresponding region in the material. Then, $H_{kj}=H_j$, where H_j is the field at the jth experimental point. Figure 5 is a representation of three experimental points at the fields H_{i-1}, H_i, and H_{i+1} which define two parts in the figure: parts I and II. In part I of Fig. 5, the measured uniaxial torque amplitude T_u follows Eq. (5). At the field H_i, the ith anisotropic region saturates and the expression for T_u in part II of the graphic will be

$$T_u=a_{i+1}+b_{i+1}H=K_1f_1+K_2f_2+\cdots+K_if_i+\left(\frac{K_{i+1}f_{i+1}}{H_{i+1}}+\cdots+\frac{K_nf_n}{H_n}\right)H. \tag{6}$$

Subtracting the slope of Eq. (6) from the slope of Eq. (5), we get

$$b_i-b_{i+1}=\frac{K_if_i}{H_i}, \tag{7}$$

then, we can obtain the contribution of the ith region to the anisotropy constant of the whole sample as

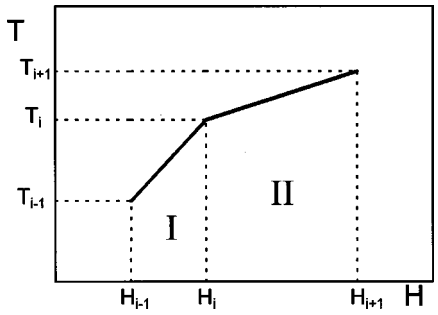

FIG. 5. Scheme corresponding to three hypothetical $T-H$ experimental points. The three points form the regions I and II in the graphic. The change in the slope that occurs at the central point is due to the saturation of a certain volume in the sample that exhibits a magnetic anisotropy with anisotropy field equal to H_i.

$$K_i f_i = (b_i - b_{i+1}) H_i . \tag{8}$$

Looking at Fig. 5 we can write the slopes as a function of the magnetic fields H_i and torque amplitudes T_i of each experimental point

$$b_i = \frac{T_i - T_{i-1}}{H_i - H_{i-1}}, \tag{9}$$

$$b_{i+1} = \frac{T_{i+1} - T_i}{H_{i+1} - H_i}. \tag{10}$$

Taking into account of Eq. (4) and the fact that $H_{ki} = H_i$, we can obtain the volume fraction occupied by the ith anisotropic region in the following way:

$$f_i = \frac{2}{\mu_0 M_s}\left(\frac{T_i - T_{i-1}}{H_i - H_{i-1}} - \frac{T_{i+1} - T_i}{H_{i+1} - H_i}\right). \tag{11}$$

By means of Eqs. (4) and (11) and the experimental data (H_i, T_i), it is possible to make an evaluation of the anisotropy distribution in the volume of the material. Evidently, this evaluation will be more accurate when more experimental points have been measured, mainly in the nonlinear zones of the curves.

We have applied the model to the torque results shown in Figs. 2 and 3 taking into account the following points:

The saturation induction $\mu_0 M_s$ of VITROVAC 6150 is 1 T and for $Co_{66}B_{12}Si_{16}Fe_4Mo_2$, it is 0.55 T.

According to the dimensions of the samples and the values of the saturation magnetization, we have estimated demagnetizing fields of 45 Oe for VITROVAC 6150 and 20 Oe for $Co_{66}B_{12}Si_{16}Fe_4Mo_2$.

We have evaluated the effective magnetic field inside the samples by correcting the applied magnetic field with the demagnetizing field.

The results of the model applied to the torque experimental data of VITROVAC 6150 and $Co_{66}B_{12}Si_{16}Fe_4Mo_2$ are presented in Tables I and II, respectively. The tables are divided into three blocks. The first block shows the estimated internal magnetic field and the corresponding magnetic anisotropy K_i. The anisotropy constant K_i is calculated assuming the magnetic field to be the anisotropy field of the ith zone in which we divide the volume of the sample in order to apply the model.

In the second block, we present the results for the nontreated samples (as-cast). The first column collects the values of the uniaxial torque amplitude T_u measured by means of the torque magnetometer. The second column shows the values of the volume fraction f_i of the zone in the sample affected by the magnetic anisotropy with value K_i. The last column contains the contribution of each zone to the total uniaxial torque amplitude measured in the torque magnetometer. This contribution is calculated as the product $f_i K_i$.

The third block shows the results obtained after the mechanical polishing of the samples and it has the same layout as the second block.

Looking at the two tables we can point out the following general characteristics:

TABLE I. Anisotropy distribution of VITROVAC 6150 in the as-quenched state and after the mechanical polishing.

		As quenched			After mechanical polishing		
$\mu_0 H$ (T)	K_i (J m^{-3})	T_u (J m^{-3})	$f_1(10^{-2})$	$f_i K_i$	T_u (J m^{-3})	$f_i(10^{-2})$	$f_i K_i$
0.9955	396000	322	0.000	0.00	236	0.000	0.00
0.7955	317000	322	0.002	7.56	236	0.001	2.42
0.4955	197000	319	0.007	13.9	235	0.001	1.51
0.2455	97700	310	0.017	16.7	233	0.009	8.96
0.1455	57900	299	0.031	17.8	229	0.009	5.31
0.0955	38000	288	0.036	13.6	225	0.026	9.87
0.0655	26100	277	0.050	13.1	220	0.004	1.00
0.0455	18100	265	0.057	10.4	216	0.011	2.08
0.0255	10100	249	0.113	11.4	211	0.044	4.46
0.0175	6960	239	0.116	8.10	207	0.010	0.67
0.0135	5370	233	0.090	4.81	206	0.076	4.10
0.0095	3780	224	0.161	6.09	202	0.115	4.33
0.0075	2980	219	0.329	9.83	200	0.122	3.63
0.0055	2190	211	0.093	2.04	197	0.177	3.87
0.0035	1390	202	1.14	15.9	192	0.731	10.2
0.0015	597	184	28.6	171	181	29.0	173

TABLE II. Anisotropy distribution of $Co_{66}B_{12}Si_{16}Fe_4Mo_2$ in the as-quenched state and after the mechanical polishing.

		As quenched			After mechanical polishing		
$\mu_0 H$ (T)	K_i (J m^{-3})	T_u (J m^{-3})	$f_i(10^{-2})$	$f_i K_i$	T_u (J m^{-3})	$f_i(10^{-2})$	$f_i K_i$
0.998	218000	108	0.006	12.1	12.4	0.000	0.00
0.798	175000	105	0.006	10.7	12.4	0.000	0.03
0.498	109000	98	0.016	17.8	12.3	0.002	1.85
0.248	54300	82	0.025	13.8	11.4	0.001	0.72
0.148	32400	71	0.028	9.0	10.7	0.001	0.33
0.098	21500	62	0.029	6.3	10.3	0.005	1.05
0.068	14900	54	0.038	5.6	9.7	0.001	0.14
0.048	10500	48	0.036	3.7	9.3	0.016	1.63
0.028	6130	40	0.089	5.5	8.2	0.009	0.56
0.018	3940	34	0.070	2.8	7.4	0.045	1.76
0.014	3060	31	0.157	4.8	6.7	0.012	0.37
0.01	2190	27	0.147	3.2	5.9	0.005	0.11
0.008	1750	24	0.214	3.7	5.5	0.168	2.95
0.005	1090	18.2	0.154	1.7	3.7	0.042	0.46
0.003	657	13.7	0.955	6.3	2.4	0.002	0.01
0.001	219	5.1	0.362	0.79	1.1	0.171	0.38

(1) Regions with higher anisotropy occupy, in general, smaller volume fractions.

(2) Although the regions with anisotropy of the order of 10^4-10^5 J m^{-3} have volume fractions smaller than 0.10%, they contribute appreciably to the total anisotropy of the samples. In the case of $Co_{66}B_{12}Si_{16}Fe_4Mo_2$, these high anisotropies contribute even more than the low anisotropies that occupy greater volume fractions.

From Tables I and II, it is also possible to observe a great difference between the anisotropy distributions of the two samples, namely, the remarkably large volume that the low anisotropy zones occupy in the sample VITROVAC 6150, about 1% of the volume has a uniaxial anisotropy of about 1200 J m^{-3} and 29% exhibits a magnetic anisotropy of 600 J m^{-3}. It seems evident that in the case of VITROVAC 6150 the bulk of the amorphous alloy has a weak magnetic anisotropy (less than 600 J m^{-3}).

This low anisotropy affecting the bulk of the sample can be attributed to the existence of directional order in the material. The pair ordering would be induced during the manufacturing process in materials with high Curie temperature as was shown in previous works.[5,9]

In VITROVAC 6150, zones with magnetic anisotropy up to 2000 J m^{-3} occupy a 29.8% of the volume and contribute 188.7 J m^{-3} to the total anisotropy. After mechanical polishing, the same zones occupy 29.9% and contribute 187.3 J m^{-3}. This fact indicates that surface roughness is not the main origin of the anisotropy present in the corresponding zones of the sample.

The fact that small anisotropies do not change with mechanical polishing indicates that they are homogeneously distributed throughout the whole material. This reinforces the idea that they are produced by the existence of directional order in the alloy VITROVAC 6150.

In the case of $Co_{66}B_{12}Si_{16}Fe_4Mo_2$, there is no volume fraction above 1%, to which an anisotropy of about 700 J m^{-3} may correspond. In this case, the amorphous bulk of the material does not seem to have an appreciable magnetic anisotropy.

The absence of appreciable magnetic anisotropy in the bulk of the sample of $Co_{66}B_{12}Si_{16}Fe_4Mo_2$ is confirmed by the fact that the magnetic anisotropy diminishes by 90% after mechanical polishing of the sample. It is evidence that surface roughness is the main origin of the magnetic anisotropy. Finally, the small volume fractions obtained are in accordance with the part of the volume occupied by surface roughness.

Figures 6 and 7 show the magnetization curves of the circular samples of VITROVAC 6150 and $Co_{66}B_{12}Si_{16}Fe_4Mo_2$, respectively, in the as-quenched state. Each figure shows the magnetization curve along the longitudinal direction (which is the direction of easy magnetization) and along the transversal one. Observing Figs. 6 and 7, we can emphasize the following facts:

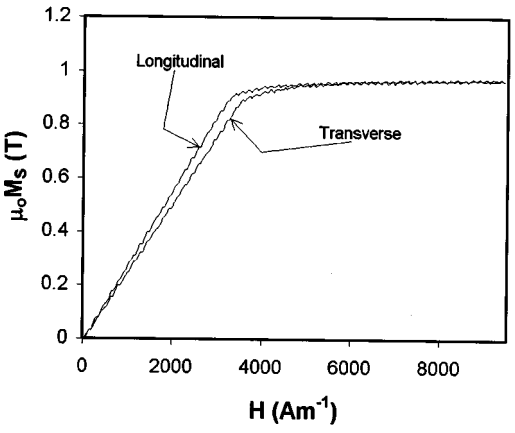

FIG. 6. Magnetization curves of VITROVAC 6150 along the longitudinal and transverse directions.

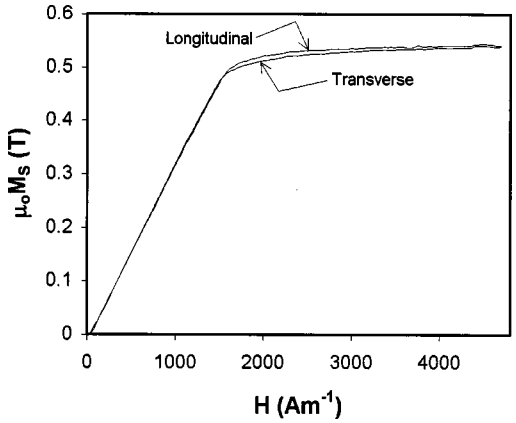

FIG. 7. Magnetization curves of $Co_{66}B_{12}Si_{16}Fe_4Mo_2$ along the longitudinal and transverse directions.

(1) In VITROVAC 6150 (Fig. 6), the magnetization curve along the longitudinal direction has a higher slope than the curve along the transversal direction. At about 3000 $A\,m^{-1}$, both magnetization curves bend and become practically horizontal with the transversal magnetization slightly lower than the longitudinal one. The area enclosed by the two magnetization curves at these low applied magnetic fields was estimated by the graphical method as 170 $J\,m^{-3}$.

(2) In $Co_{66}B_{12}Si_{16}Fe_4Mo_2$ (Fig. 7), the magnetization curves along the longitudinal and transversal directions practically coincide at low fields, and above 1600 $A\,m^{-1}$ the two curves become practically horizontal, but the magnetization curve along the transversal direction is now always under the curve corresponding to the longitudinal direction. In this case, the curves do not enclose an appreciable area at these low fields.

The area enclosed by the two magnetization curves is a good approximation of the uniaxial anisotropy present in the plane of the sample. Then, the value of 170 $J\,m^{-3}$ calculated approximately from the area enclosed by the magnetization curves of VITROVAC 6150 at low fields could be related to the contribution to the anisotropy due to the zones in the sample exhibiting low anisotropy fields.

As was pointed out before in VITROVAC 6150, the zones with magnetic anisotropy less than 2000 $J\,m^{-3}$ (H_a up to 4000 $A\,m^{-1}$) contribute 181 $J\,m^{-3}$ to the total anisotropy. This value is in good agreement with that obtained from the magnetization curves. In the case of $Co_{66}B_{12}Si_{16}Fe_4Mo_2$, there is no difference between the magnetization curves along the longitudinal and transverse directions. This result is in agreement with the fact that the bulk of this sample is essentially isotropic. In this case, its anisotropy cannot be evaluated from the difference between the magnetization curves because this difference exists mainly in the region of high applied magnetic fields.

IV. CONCLUSION

In this article, torque measurements of the macroscopic in-plane magnetic anisotropy for two Co-based amorphous alloys (VITROVAC 6150 and $Co_{66}B_{12}Si_{16}Fe_4Mo_2$) are presented. A different behavior was observed in the approach to saturation of the uniaxial torque amplitude T_u with the applied magnetic field. In order to explain this difference, a simple model has been developed, in which the amorphous samples are supposed to be formed by a certain number of regions exhibiting different magnetic anisotropy constants and occupying different volume fractions within the sample. In other words, the macroscopic anisotropy is the volume average of the anisotropy distribution throughout the amorphous material.

For VITROVAC 6150, the measurements are interpreted by the model to indicate that this material exhibits a kind of magnetic anisotropy that affects the bulk of the sample. This anisotropy may be due to the presence of pair ordering in the sample. The magnetization curves in the longitudinal and transverse directions of this sample show different slopes at low magnetic fields. The two magnetization curves enclose an area of about 170 $J\,m^{-3}$ that is related to the magnetic anisotropy in the plane of the sample and it is in good agreement with the contribution of the low anisotropy regions to the total magnetic anisotropy, which is 190 $J\,m^{-3}$.

On the other hand, the sample of $Co_{66}B_{12}Si_{16}Fe_4Mo_2$ shows an anisotropy distribution characterized by the presence of more intense magnetic anisotropies, but occupying very small volume fractions. In this case, the bulk of the material is essentially isotropic. The origin of the macroscopic in-plane magnetic anisotropy for this alloy should be due mainly to the magnetostatic effect of the surface roughness. This conclusion is confirmed by the fact that the magnetic anisotropy diminishes by as much as a 90% when the roughness of the wheel surface is removed by mechanical polishing. The magnetization curves along the longitudinal and transversal direction in this case do not enclose any significant area at low fields.

ACKNOWLEDGMENT

This work was supported in part by the CICYT under the Grant No. 96-0667, Madrid, Spain.

[1] L. Kraus, I. Tomás, E. Kratochvilová, B. Springmann, and E. Müller, Phys. Status Solidi A **100**, 289 (1987).
[2] M. Takahashi and S. Ishio, Jpn. J. Appl. Phys., Part 1 **29**, 129 (1979).
[3] H. N. Ok and A. H. Morrish, Phys. Rev. B **23**, 2257 (1981).
[4] H. Morita, H. Fujimori, and Y. Obi, Jpn. J. Appl. Phys., Part 1 **18**, 683 (1979).
[5] M. Tejedor, J. A. García, and J. Carrizo, J. Magn. Magn. Mater. **131**, 329 (1994).
[6] J. S. Kouvel and C. D. Graham, J. Appl. Phys. **28**, 340 (1957).
[7] R. F. Krause and B. D. Cullity, J. Appl. Phys. **39**, 5532 (1968).
[8] M. Tejedor, J. A. García, and J. Carrizo, J. Magn. Magn. Mater. **118**, 333 (1993).
[9] M. Tejedor, J. A. García, and J. Carrizo, J. Magn. Magn. Mater. **117**, 141 (1992).